Crystals 2022

MDPI

Proceedings

Fabrication and characterization of perovskite solar cells using copper phthalocyanine complex with tetracyanoquinodimethane†

Atsushi Suzuki[1]*, Ryota Hasegawa[1], Takeo Oku[1], Masanobu Okita[2], Sakiko Fukunishi[2], Tomoharu Tachikawa[2], and Tomoya Hasegawa[2]

[1] The University of Shiga Prefecture, 2500 Hassaka, Hikone, Shiga 522-8533, Japan, suzuki@mat.usp.ac.jp, oe21rhasegawa@ec.usp.ac.jp, oku@mat.usp.ac.jp
[2] Osaka Gas Chemicals Co., Ltd., 5-11-61 Torishima, Konohana-ku, Osaka 554-0051, Japan okita@ogc.co.jp; fukunishi@ogc.co.jp; t-tachikawa@ogc.co.jp; hasegawa_tomoya@ogc.co.jp
* Correspondence: suzuki@mat.usp.ac.jp; Tel. +81-749-28-8369 (A. S.)
† Presented at the title, place, and date.

Abstract: Fabrication and characterization of $CH_3NH_3PbI_3$ perovskite solar cells using decaphenylpentacyclosilane, copper phthalocyanine complex (CuPc) doped with tetracyanoquinodimethane (TCNQ) were performed. Effects of carboxylic acid, amino or sulfonic acid sodium salt group substituted with CuPc doped with TCNQ on the photovoltaic properties were investigated for improving the carrier generation and diffusion related to short circuit current density. Incorporation of carboxylic acid or amino-substituted with CuPc doped with TCNQ would optimize tuning energy levels of valence band, promoting charge transfer and diffusion with suppressing trap near the interface in the hole-transporting layer.

Keywords: perovskite solar cell; phthalocyanine; tetracyanoquinodimethane; photovoltaic properties; morphology

1. Introduction

Perovskite solar cells have a high potential to apply for practical use of photovoltaic devices such as solar cell with characteristics such as high-power conversion efficiency as the photovoltaic performance and easy manufacturing process [1-4]. The perovskite solar cells were constructed with photo-active layer on hole-transporting layers [5]. The photovoltaic properties were based on the perovskite crystal and chemical elements such as organic cation; methyl ammonium (MA) [6], ethyl ammonium (EA) [7, 8], formamidinium (FA) [9, 10], guanidinium (GA) [11-13], phenyl ethyl ammonium (PEA) [14], *p*-phenylenediaminium [15], alkali metals (sodium, potassium, rubidium or cesium) [16, 17] at A-site, lead [18], tin, transition metals [19-21], lanthanide or rare earth ions [22, 23] at B-site and halogen anion at X-site in perovskite crystal. The photovoltaic characteristics of the perovskite crystals with tuning composition mole-ratio of chemical elements have been performed for improving the conversion efficiency, the morphologies and crystal orientation. The photovoltaic performances are based on carrier diffusion with suppression of recombination and trapping near defect and interfaces between crystal grains in the perovskite layer. The stability of the photovoltaic performance was performed for suppressing desorption of the organic cation and halogen anion. Partial substitution of organic cation, transition and alkali metals, and halogen atom, development of alternative hole-transporting materials were performed for applying the photovoltaic devices.

Alternative hole-transporting materials using silane derivatives such as decaphenylcyclopentasilane (DPPS) in terms of conventional hole-transporting material such as 2,2′,7,7′-tetrakis(*N*,*N*-di-*p*-methoxyphenylamine)-9,9′-spirobifluorene (spiro-OMeTAD) have been developed for improving stability of the conversion efficiency while suppressing the decomposition. [24, 27-31]. In addition, metal phthalocyanines as organic semi-conductive materials have

Citation: Lastname, F.; Lastname, F.; Lastname, F. Title. *Chem. Proc.* **2021**, *3*, x. https://doi.org/10.3390/xxxxx

Published: date

advantage to apply the electronic devices such as organic solar cell and perovskite solar cells [32-41]. The photovoltaic properties of the metal phthalocyanine complex were based on electron structure and molecular modification. Addition of the metal phthalocyanines into the perovskite layer promoted the photo-induced carrier generation, charge diffusion related to mobility with optimization of the surface morphology on the perovskite layer. Optimization with tuning the microstructure and morphologies in the perovskite layer is important factor for improving the stability of the conversion efficiency. Metal phthalocyanine complexes derivatives (MPc, M = Cu^{2+}, Zn^{2+}) doped with 7,7,8,8-tetracyanoquinodimethane (TCNQ) were used as efficient hole-transporting material for improving the carrier mobility related to short circuit current density and conversion efficiency [42].

The purpose of this study is to fabricate and characterize the perovskite solar cells using DPPS with addition of cupper phthalocyanine complex derivatives ($CuPcX_4$) doped with TCNQ as hole-transporting materials. Especially, influence of carboxylic acid, amino or sulfonic acid sodium salt group substituted with CuPc doped with TCNQ on the photovoltaic properties were investigated. The photovoltaic properties were measured by current-voltage (*J-V*) curves under light irradiation. The photovoltaic properties were discussed by the experimental results.

2. Materials and Methods

The $CH_3NH_3PbI_3$ ($MAPbI_3$) perovskite solar cell using DPPS and MPc doped with TCNQ was fabricated as following process. For preparation of solar cell's substrate, F-doped tin oxide (FTO) substrates were cleaned using an ultrasonic bath with acetone and methanol, and dried under nitrogen gas. The 0.15 and 0.30 M TiO_x precursor solution was prepared from titanium diisopropoxide bis(acetylacetonate) (0.055 and 0.11 mL, Sigma-Aldrich, Tokyo, Japan) with 1-butanol (1 mL, Nacalai Tesque, Kyoto, Japan), and the 0.15 M TiO_x precursor solution was spin-coated on the FTO substrate at 3000 rpm for 30 s and annealed at 125 °C for 5 min. Then, the 0.30 M TiO_x precursor solution was spin-coated on the TiO_x layer at 3000 rpm for 30 s and annealed at 125 °C for 5 min. This process of 0.30 M solution was performed two times, and the FTO substrate was sintered at 500 °C for 30 min to form the compact TiO_2 layer. After that, TiO_2 paste was coated on the substrate by spin-coating at 5000 rpm for 30 s. For the formation of mesoporous TiO_2 layer, the TiO_2 paste was prepared with TiO_2 powder (P-25, Aerosil, Tokyo, Japan) with polyethylene glycol (PEG #20000, Naalai Tesque, Kyoto, Japan) in ultrapure water. The solution was mixed with acetylacetone (10 μL, Fujifilm Wako Pure Chemical Corporation, Osaka, Japan) and triton X-100 (5 μL, Sigama Aldrich, Tokyo, Japan) for 30 min, and was left for 12 h to suppress the bubbles in the solution. The cells were annealed at 120 °C for 5 min and at 500 °C for 30 min to form the mesoporous TiO_2 layer.

For the preparation of the perovskite compounds, a solution of CH_3NH_3I (MAI, 2.4 M, Tokyo Chemical Industry, Tokyo, Japan), and PbI_2 (0.8 M, Sigma Aldrich, Tokyo, Japan) with a desired mole ratio in N, N-dimethylformanide (0.5 mL, Sigma Aldrich, Tokyo, Japan) was mixed at 60 °C. The solution of perovskite compound was then introduced into the TiO_2 mesoporous by a spin-coating method. At last stage of the spin coating, DPPS (OGSOL SI-30-15, Osaka Gas Chemicals, Osaka, Japan) as a hole-transport layer (HTL) was prepared using chlorobenzene (0.5 mL, Fujifilm Wako Pure Chemical Corporation, Osaka, Japan). The DPPS solutions were dropped on the perovskite layer during the last 15 s of spin-coating methods of the perovskite precursor solutions. The perovskite cells coated with DPPS layer were annealed at 190 °C for 10 min.

As shown in Fig. 1., cupper (II) phthalocyanine complexes were used for preparation of the hole-transporting layer. A solution of copper (II) phthalocyanine tetracarboxylic acid ($CuPc(COOH)_4$, Orient Chemical Industries Co. Ltd. Osaka, Japan), copper (II) tetra(amino)phthalocyanine ($CuPc(NH_2)_4$, Orient Chemical Industries Co. Ltd. Osaka, Japan), copper (II) phthalocyanine-tetra sulfonic acid tetrasodium salt ($CuPc(SO_3Na)_4$, 18 mg, Sigma-Aldrich, Japan) mixed with TCNQ (2 mg, Sigma-Aldrich, Japan) in ethanol (1.0 mL, Nacalai Tesque, Kyoto, Japan) was prepared by spin-coating annealing at 110 °C for 10 min. As preparation of standard hole-transporting layer, a solution of 2,2′,7,7′-tetrakis[N,N-di(methoxyphenyl)amino]-9,9′-spirobifluorene (spiro-OMeTAD, 36.1 mg, Sigma Aldrich, Tokyo, Japan) in chlorobenzene (0.5 mL, Fujifilm Wako Pure Chemical Corporation, Osaka, Japan) was mixed with a solution of lithium bis(trifluoromethylsulfonyl)imide (Li-TFSI, 260 mg, Tokyo Chemical Industry, Tokyo, Japan) in acetonitrile (0.5 mL, Sigma Aldrich, Tokyo, Japan) for 24 h. The former solution with 4-tert-butylpyridine (14.4 μL, Sigma Aldrich, Tokyo, Japan) was mixed with the Li-TFSI solution (8.8 μL) for 30 min at 70 °C. All procedures were carried out in ordinary air. Finally, gold (Au)

metal contacts were evaporated as top electrodes. Layered structures of the present photovoltaic cells were denoted as FTO/TiO_2/perovskite/DPPS/CuPc doped TCNQ/Au.

The *J–V* characteristics (Keysight B2901A, Keysight Technologies, Santa Rosa, CA, USA) of the photovoltaic cells were measured under illumination at 100 mW cm^{-2} by using an AM 1.5 solar simulator (San-ei Electric XES-301S, Osaka, Japan). One substrate was fabricated and characterized for the photovoltaic performance. The best and average conversion efficiencies, and standard deviations of the solar cells with the three electrodes prepared in this study were measured in the reverse scan of the *J-V* curves. The solar cells were illuminated through the side of the FTO substrates, and the illuminated area was 0.090 cm^2.

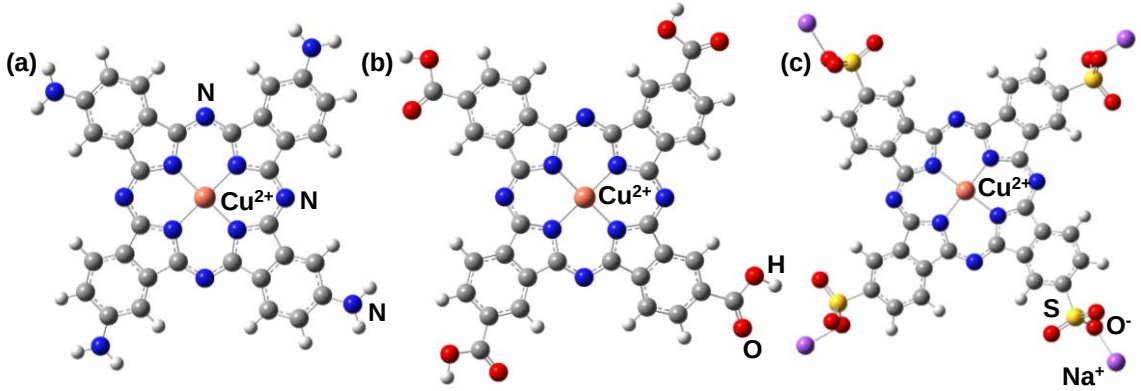

Table 1. Molecular structures of cupper (II) phthalocyanine complexes. (a) $CuPc(NH_2)_4$, (b) $CuPc(COOH)_4$, (c) $CuPc(SO_3Na)_4$.

3. Results and Discussion

The *J–V* characteristics of the photovoltaic cells were measured as listed in Table 1. In the case of $CuPc(COOH)_4$ doped with TCNQ, the photovoltaic parameters such as short-circuit current density (J_{SC}), fill factor (*FF*), series resistance (R_S), shunt resistance (R_{Sh}) and conversion efficiency (η) were obtained to be 16.8 mA cm^{-2}, 0.655 V, 0.491, 3.14 Ω cm^2, 152 Ω cm^2, and 5.49 %, as listed in Table 1. The photovoltaic performance were improved by incorporation of $CuPc(COOH)_4$ doped with TCNQ, as compared with the photovoltaic parameters in other cases. In the case of $CuPc(NH_2)_4$ doped with TCNQ, the photovoltaic performance of η decreased to be 3.76 %. In the case of $CuPc(SO_3Na)_4$ doped with TCNQ, the photovoltaic parameters of J_{sc} and V_{oc} decreased to be 2.66 mA cm^{-2} and 0.603 V, decreasing η of 0.75%. The *J–V* characteristics of the photovoltaic cells were measured after 30 days. In the all cases after 30 days, the photovoltaic parameters of J_{sc}, V_{oc}, and *FF* related to η were influenced by incorporation of $CuPcX_4$ doped with TCNQ. Especially, incorporation of $CuPc(NH_2)_4$ doped with TCNQ improved the photovoltaic parameters of V_{oc}, FF, R_S, and R_{Sh}, increasing η in the range of 6.41-6.55 % after 30 days. The incorporation of $CuPc(NH_2)_4$ doped with TCNQ have advantage to take a roll of the hole-transporting layer with remaining stability of η, instead of conventional hole-transporting material using spiro-OMeTAD.

Table 1. Photovoltaic parameters of the perovskite solar cells as prepared.

Devices	J_{SC} (mA cm^{-2})	V_{OC} (V)	FF	R_S (Ω cm^2)	R_{Sh} (Ω cm^2)	η (%)	η_{ave} (%)
$CuPc(NH_2)_4$-TCNQ	8.39	0.716	0.626	6.90	5000	3.76	1.30
$CuPc(COOH)_4$-TCNQ	16.8	0.655	0.491	3.14	152	5.49	4.45
$CuPc(SO_3Na)_4$-TCNQ	2.66	0.603	0.465	11.6	1160	0.75	0.54

The photovoltaic properties depends on the carrier diffusion while suppressing recombination near interface between the crystal grains in the perovskite layer. When incorporation of $CuPcX_4$ doped with TCNQ were performed, the carrier generation and charge transfer promoted with suppression of recombination near interface in the hole-transporting layer. The holes in the valence band of the perovskite layer charge-transferred the valence bands of DPPS, $CuPcX_4$ and TCNQ in hole-transporting layer at the Au electrode as the cathode. The valence bands of the hole-transporting layer were tuned by incorporation of $CuPcX_4$ with electronic donating and withdrawing substitution. The carboxyl acid or amino-substituted with CuPc doped with TCNQ optimized the energy levels of valence band state, promoting charge transfer and diffusion with

suppression of trap near the interface in the hole-transporting layer. The V_{oc} of the perovskite solar cells were associated with the energy gap between the valence band of the perovskite layer and the conduction band of TiO_2 as an electron-transporting layer. The incorporation of $CuPc(NH_2)_4$ doped with TCNQ improved the carrier diffusion while suppression of decomposition in the perovskite layer, yielding increase of J_{SC} related to η. As compared to the conventional fabrication using spiro-OMeTAD, the fabrication method with incorporation of $CuPcX_4$ doped with TCNQ have great advantage for applying the photovoltaic devices while having term durability of performance.

4. Conclusion

Fabrication and characterization of the perovskite solar cells using DPPS with addition of $CuPcX_4$ doped with TCNQ were performed for improving the stability of conversion efficiency. Effects of carboxylic acid, amino or sulfonic acid sodium salt group substituted with CuPc doped with TCNQ on the photovoltaic properties were investigated for improving the parameters of J_{SC} and V_{oc} related to η. Incorporation of carboxylic acid or amino substituted with CuPc doped with TCNQ would optimize tuning the energy levels of valence band state, promoting the charge transfer and diffusion while suppressing trap near the interface in the hole-transporting layer. Especially, the incorporation of $CuPc(NH_2)_4$ doped with TCNQ improved the stability of η while suppression of decomposition in the perovskite layer.

Author Contributions: For research articles with several authors, a short paragraph specifying their individual contributions must be provided. The following statements should be used "Conceptualization, A.S. and T.O.; methodology, R.H.; software, A.S.; validation, A.S., R.H. and T.O.; formal analysis, R.H.; investigation, R.H.; resources, R.H.; data curation, R.H.; writing—original draft preparation, A.H.; writing—review and editing, T.O.; visualization, R. H.; supervision, T.O.; project administration, T.O.; funding acquisition, A.S. and T.O.

Funding: This research was supported by JSPS KAKENHI Grant Number JP 21K05261.

Conflicts of Interest: The authors declare no conflict of interest.

Acknowledgement: We wish to thank Dr. Yasuhiro Yamazaki belonging to Orient Chemical Industries Co. Ltd. for suppling cupper phthalocyanine complex as the hole-transforming materials

References

1. Yoo J.J.; Seo G.; Chua M.R.; Park T.G.; Lu Y.; Rotermund F.; Kim Y.K.; Moon C.S.; Jeon N.J.; Baena J.P.C.; Bulović V.; Shin S.S.; Bawendi M.G.; Seo J., Efficient perovskite solar cells via improved carrier management, *Nature*, **2021**, *590*, pp. 587–593. https://doi.org/10.1038/s41586-021-03285-w
2. Jeong J.; Kim M.; Seo J.; Lu H.; Ahlawat P.; Mishra A.; Yang Y.; Hope M.A.; Eickemeyer F.T.; Kim M.; Yoon Y.J.; Choi I.W.; Darwich B.P.; Choi S.J.; Jo Y.; Lee J.H.; Walker B.; Zakeeruddin S.M.; Emsley L.; Rothlisberger U.; Hagfeldt A.; Kim D.S.; Grätzel M.; Kim J.Y., Pseudo-halide anion engineering for α-$FAPbI_3$ perovskite solar cells, *Nature*, **2021**, *592*, pp. 381–385. https://doi.org/10.1038/s41586-021-03406-5
3. Dong Q.; Zhu C.; Chen M.; Jiang C.; Guo J.; Feng Y.; Dai Z.; Yadavalli S.K.; Hu M.; Cao X.; Li Y.; Huang Y.; Liu Z.; Shi Y.; Wang L.; Padture N.P.; Zhou Y., Interpenetrating interfaces for efficient perovskite solar cells with high operational stability and mechanical robustness. *Nat. Commun* **2021**, *12*, pp. 973. https://doi.org/10.1038/s41467-021-21292-3
4. Kim D.; Jung H.J.; Park I.J.; Larson B.W.; Dunfield S.P.; Xiao C.; Kim J.; Tong J.; Boonmongkolras P.; Ji S.G.; Zhang F.; Pae S.R.; Kim M.; Kang S.B.; Dravid V.; Berry J.J.; Kim J.Y.; Zhu K.; Kim D.H.; Shin B., Efficient, stable silicon tandem cells enabled by anion-engineered wide-bandgap perovskites, *Science*, **2020**, 368, pp. 155–160. https://doi.org/10.1126/science.aba3433
5. Gao B.; Meng J., RbCs(MAFA)PbI_3 perovskite solar cell with 22.81% efficiency using the precise ions cascade regulation, *Appl. Sur. Sci.* **2020**, *530*, pp. 147240. https://doi.org/10.1016/j.apsusc.2020.147240
6. Sun P.P.; Kripalani D.R.; Chi W.; Snyder S.A.; Zhou K., High carrier mobility and remarkable photovoltaic performance of two-dimensional Ruddlesden–Popper organic–inorganic metal halides $(PA)_2(MA)_2M_3I_{10}$ for perovskite solar cell applications, *Material Today*, **2021**, *47*, pp. 45-52. https://doi.org/10.1016/j.mattod.2021.02.007
7. Liu Z.; Qiu L.; Ono L.K.; He S.; Hu Z.; Jiang M.; Tong G.; Wu Z.; Jiang Y.; Son D.Y.; Dang Y.; Kazaoui S.; Qi Y., A holistic approach to interface stabilization for efficient perovskite solar modules with over 2,000-hour operational stability, *Nature Energy*, **2020**, *5*, pp. 596–604. https://doi.org/10.1038/s41560-020-0653-2
8. Nishi K.; Oku T.; Kishimoto T.; Ueoka N.; Suzuki A., Photovoltaic characteristics of $CH_3NH_3PbI_3$ perovskite solar cells added with ethyl ammonium bromide and formamidinium iodide, *Coating*, **2020**, *10*, 410. https://doi.org/10.3390/coatings10040410

9. Lyu M.; Park N.G., Effect of additives AX (A = FA, MA, Cs, Rb, NH_4, X = Cl, Br, I) in $FAPbI_3$ on photovoltaic parameters of perovskite solar cells, *RRL Solar* **2021**, *4(10)*, 2000331. https://doi.org/10.1002/solr.202000331
10. Kim G.; Min H.; Lee K.S.; Lee D.Y.; Yoon S.M.; Seok S.Il., Impact of strain relaxation on performance of α-formamidinium lead iodide perovskite solar cells, *Science* **2020**, *370*, pp. 108–112. https://doi.org/10.1126/science.abc4417
11. Gao L.; Li X.; Liu Y.; Fang J.; Huang S.; Spanopoulos I.; Li X.; Wang Y.; Chen L.; Yang G.; Kanatzidis M.G., Incorporated guanidinium expands the $CH_3NH_3PbI_3$ lattice and enhances photovoltaic performance, *ACS Appl. Mater. Interfaces* **2020**, *12(39)*, pp. 43885–43891. https://doi.org/10.1021/acsami.0c14925
12. Chavan R.D.; Prochowicz D.; Tavakoli M.M.; Yadav P.; Hong C.K., Surface treatment of perovskite layer with guanidinium iodide leads to enhanced moisture stability and improved efficiency of perovskite solar cells, *Adv. Mater. Interfaces*, **2020**, *7*, pp. 2000105. https://doi.org/10.1002/admi.202000105
13. Kishimoto T.; Suzuki A.; Ueoka N.; Oku T., Effects of guanidinium addition to $CH_3NH_3PbI_{3-x}Cl_x$ perovskite photovoltaic devices, *J. Ceram. Soc. Jpn.* **2019**, *127*, pp. 491-497. https://doi.org/10.2109/jcersj2.18214
14. Liu C.; Yang Y.; Rakstys K.; Mahata A.; Franckevicius M.; Mosconi E.; Skackauskaite R.; Ding B.; Brooks K.G.; Usiobo O.J.; Audinot J.N.; Kanda H.; Driukas S.; Kavaliauskaite G.; Gulbinas V.; Dessimoz M.; Getautis V.; Angelis F.D.; Ding Y.; Dai S.; Dyson P.J.; Nazeeruddin M.K., Tuning structural isomers of phenylenediammonium to afford efficient and stable perovskite solar cells and modules, *Nat. Commun.* **2021**, *12*, pp. 6394. https://doi.org/10.1038/s41467-021-26754-2
15. Zardari P.; Rostami A.; Shekaari H., p-Phenylenediaminium iodide capping agent enabled self-healing perovskite solar cell, *Sci. Rep.* **2020**, *10,* pp. 20011. https://doi.org/10.1038/s41598-020-76365-y
16. Dong Q.; Zhu C.; Chen M.; Jiang C.; Guo J.; Feng Y.; Dai Z.; Yadavalli S.K.; Hu M.; Cao X.; Li Y.; Huang Y.; Liu Z.; Shi Y.; Wang L.; Padture N.P.; Zhou Y., Interpenetrating interfaces for efficient perovskite solar cells with high operational stability and mechanical robustness, *Nat. Commun.* **2021**, *12*, pp. 973. https://doi.org/10.1038/s41467-021-21292-3
17. Chen Y., Li N., Wang L., Li L., Xu Z., Jiao H., Liu P., Zhu C., Zai H., Sun M., Zou W., Zhang S., Xing G., Liu X., Wang J., Li D., Huang B., Chen Q., Zhou H., Impacts of alkaline on the defects property and crystallization kinetics in perovskite solar cells, *Nat. Commun.* **2019**, *10*, pp. 1112. https://doi.org/10.1038/s41467-019-09093-1
18. Li C.; Song Z.; Chen C.; Xiao C.; Subedi B.; Harvey S.P.; Shrestha N.; Subedi K.K.; Chen L.; Liu D.; Li Y.; Kim Y.W.; Jiang C.; Heben M.J.; Zhao D.; Ellingson R.J.; Podraza N.J.; Jassim M.A.; Yan Y., Low-bandgap mixed tin–lead iodide perovskites with reduced methylammonium for simultaneous enhancement of solar cell efficiency and stability, *Nat. Energy*, **2020**, *5*, pp. 768–776. https://doi.org/10.1038/s41560-020-00692-7
19. Sun P.P.; Kripalani D.R.; Chi W.; Snyder S.A.; Zhou K., High carrier mobility and remarkable photovoltaic performance of two-dimensional Ruddlesden–Popper organic–inorganic metal halides $(PA)_2(MA)_2M_3I_{10}$ for perovskite solar cell applications, *Mater. Today* **2021**, 47, pp. 45-52. https://doi.org/10.1016/j.mattod.2021.02.007
20. Ueoka N.; Oku T.; Suzuki A., Additive effects of alkali metals on Cu-modified $CH_3NH_3PbI_{3-\delta}Cl_\delta$ photovoltaic devices *RSC Adv.* **2019**, *9*, 24231. https://doi.org/10.1039/c9ra03068a
21. Suzuki A.; Oku T., Effects of transition metals incorporated into perovskite crystals on the electronic structures and magnetic properties by first-principles calculation, *Heliyon* **2018**, *4*, e00755. https://doi.org/10.1016/j.heliyon.2018.e00755
22. Song Z.; Xu W.; Wu Y.; Liu S.; Bi W.; Chen X.; Song H., Incorporating of lanthanides ions into perovskite film for efficient and stable perovskite solar cells, *Small*, **2020**, *16*, 2001770. https://doi.org/10.1002/smll.202001770
23. Suzuki A.; Oku T., Effects of mixed-valence states of Eu-doped $FAPbI_3$ perovskite crystals studied by first-principles calculation, *Mater. Adv.*, **2021**, *2*, pp.2609-2616. https://doi.org/10.1039/d0ma00994f
24. Akman E.; Shalan A.E.; Sadegh F.; Akin S., Moisture-resistant $FAPbI_3$ perovskite solar cell with 22.25 % power conversion efficiency through pentafluorobenzyl phosphonic acid passivation. *ChemSusChem*, **2021**, *14(4)*, pp. 1176-1183. https://doi.org/10.1002/cssc.202002707
25. Zhu H.; Shen Z.; Pan L.; Han J.; Eickemeyer F.T.; Ren Y.; Li X.; Wang S.; Liu H.; Dong X.; Zakeeruddin S.M.; Hagfeldt A.; Liu Y.; Grätzel M., Low-cost dopant additive-free hole-transporting material for a robust perovskite solar cell with efficiency exceeding 21%, *ACS Energy Lett.* **2021**, *6(1)*, pp. 208–215. https://doi.org/10.1021/acsenergylett.0c02210
26. Wan L.; Zhang W.; Fu S.; Chen L.; Wang Y.; Xue Z.; Tao Y.; Zhang W.; Song W.; Fang J., Achieving over 21% efficiency in inverted perovskite solar cells by fluorinating a dopant-free hole transporting material, *J. Mater. Chem. A*, **2020**, *8*, pp. 6517-6523. https://doi.org/10.1039/D0TA00522C
27. Jeong M.; Choi I.W.; Go E.M.; Cho Y.; Kim M.; Lee B.; Jeong S.; Jo Y.; Choi H.W.; Lee J.; Bae J.H.; Kwak S.K.; Kim D.S.; Yang C., Stable perovskite solar cells with efficiency exceeding 24.8% and 0.3-V voltage loss, *Science* **2020**, *369*, pp. 1615-1620. https://doi.org/10.1126/science.abb7167
28. Taguchi M.; Suzuki A.; Oku T.; Ueoka N.; Minami S.; Okita M., Effects of annealing temperature on decaphenylcyclopentasilane-inserted $CH_3NH_3PbI_3$ perovskite solar cells, *Chem. Phys. Lett.* **2019**, *737*, pp. 136822. https://doi.org/10.1016/j.cplett.2019.136822
29. Oku T.; Kandori S.; Taguchi M.; Suzuki A.; Okita M.; Minami S.; Fukunishi S.; Tachikawa T., Polysilane-inserted methylammonium lead iodide perovskite solar cells doped with formamidinium and potassium, *Energies* **2020**, *13*, pp. 4776. https://doi.org/10.3390/en13184776
30. Oku T.; Taguchi M.; Suzuki A.; Kitagawa K.; Asakawa Y.; Yoshida S.; Okita M.; Minami S.; Fukunishi S.; Tachikawa T., Effects of polysilane addition to chlorobenzene and high temperature annealing on $CH_3NH_3PbI_3$ perovskite photovoltaic Devices, *Coatings* **2021**, *11*, 665. https://doi.org/10.3390/coatings11060665

31. Suzuki A.; Taguchi M.; Oku T.; Okita M.; Minami S.; Fukunishi S.; Tachikawa T., Additive effects of methyl ammonium bromide or formamidinium bromide in methylammonium lead iodide perovskite solar cells using decaphenylcyclopentasilane, *J. Mater. Sci.: Mater. Electron.* **2021**, *32*, 26449–26464. https://doi.org/10.1007/s10854-021-07023-w
32. Jiang X.; Wang D.; Yu Z.; Ma W.; Li H.B.; Yang X.; Liu F.; Hagfeldt A.; Sun L., Molecular engineering of copper phthalocyanines: A Strategy in developing dopant-free hole-transporting materials for efficient and ambient-stable perovskite solar cells, *Adv. Energy Mater.* **2019**, *9*, pp. 1803287. https://doi.org/10.1002/aenm.201803287
33. Matsuo Y.; Ogumi K.; Jeon I.; Wang H.; Nakagawa T., Recent progress in porphyrin- and phthalocyaninecontaining perovskite solar cells, *RSC Adv.*, **2020**, *10*, pp. 32678–32689. https://doi.org/10.1039/d0ra03234d
34. Yu Z.; Wang L.; Mu X.; Chen C.C.; Wu Y.; Cao J.; Tang Y., Intramolecular electric field construction in metal phthalocyanine as dopant-free hole transporting material for stable perovskite solar cells with >21% efficiency, *Angew. Chem. Int. Ed.* **2021**, *60*, pp. 6294-6299. https://doi.org/10.1002/anie.202016087
35. Huang P.; Hern´andez A.; Kazim S.; Ortiz J.; Santos A.S.; Ahmad S., Molecularly engineered thienyl-triphenylamine substituted zinc phthalocyanine as dopant free hole-transporting materials in perovskite solar cells, *Sustainable Energy Fuels*, **2020**, *4*, pp. 6188–6195. https://doi.org/10.1039/d0se01215g
36. Molina D.; Preciado M.A.R.; Carlsen B.; Eickemeyer F.T.; Yang B.; Díaz N.F.; Martins M.J.Á.; Nonomura K.; Hagfeldt A.; Santos Á.S., Zinc phthalocyanine conjugated dimers as efficient dopant-free hole transporting materials in perovskite solar cells, *ChemPhotoChem*, **2020**, *4*, pp. 307-314. https://doi.org/10.1002/cptc.201900245
37. Javaidab S.; Lee G., The impact of molecular orientation on carrier transfer characteristics at a phthalocyanine and halide perovskite interface, *RSC Adv.*, **2021**, *11*, pp. 31776-31782. https://doi.org/10.1039/d1ra05909b
38. Xiao G.B.; Wang L.Y.; Mu1 X.J.; Zou X.X.; Wu Y.Y.; Cao J., Lead and iodide fixation by thiol copper(II) porphyrin for stable and environmental-friendly perovskite solar cells, *CCS Chem.* **2021**, *3*, pp. 25–36. https://doi.org/10.31635/ccschem.021.202000516
39. Huang P.; Hernández A.; Kazim S.; Berná J.F.; Ortiz J.; Lezama L.; Santos Á.S.; Ahmad S., Asymmetrically substituted phthalocyanines as dopant-free hole selective layers for reliability in perovskite solar cells, *ACS Appl. Energy Mater.* **2021**, *4*, pp. 10124–10135. https://doi.org/10.1021/acsaem.1c02039
40. Hu Q.; Rezaee E.; Xu W.; Ramachandran R.; Chen Q.; Xu H.; Assaad T.E.; McGrath D.V.; Xu Z.X., Dual defect-passivation using phthalocyanine for enhanced efficiency and stability of perovskite solar cells, *Small* **2021**, *17*, 2005216-1-12. https://doi.org/10.1002/smll.202005216,
41. Esqueda M.L.; Vergara M.E.S.; Bada J.R.Á.; Salcedo R., CuPc: Effects of its doping and a study of its organic-semiconducting properties for application in flexible devices, *Materials* **2019**, *12*, 432. https://doi.org/10.3390/ma12030434
42. Capita´n M.J.; A´lvarez J.; Naviod C., Study of the electronic structure of electron accepting cyano-films: TCNQ versus TCNE, *Phys. Chem. Chem. Phys.*, **2018**, *20*, pp. 10450-10459, https://doi.org/10.1039/c7cp07963j
43. Suzuki A.; Kida T.; Takagi T.; Oku T., "Effects of hole-transporting layers of perovskite-based solar cells", *J. J. Appl. Phys.* **2016**, *55*, 02BF01-1-5. http://doi.org/10.7567/jjap.55.02bf01
44. Suzuki A.; Okumura H.; Yamasaki Y.; Oku T., Fabrication and characterization of perovskite type solar cells using phthalocyanine complexes, *Appl. Surf. Sci.* **2019**, *488*, 586-592. https://doi.org/10.1016/j.apsusc.2019.05.305
45. Suzuki A.; Hayashi Y.; Yamasaki Y.; Oku T., Fabrication and characterization of perovskite solar cells added with zinc phthalocyanine to active layer, *AIP Conf. Proc.* **2019**, *2067*, 020010-1-6. https://doi.org/10.1063/1.5089443